Journal of Geochemical Exploration 124 (2013) 218–229

Contents lists available at SciVerse ScienceDirect

Journal of Geochemical Exploration

journal homepage: www.elsevier.com/locate/jgeoexp

Geochemical exploration using surveys of spring water, hydrocarbon and gas seepage, and geobotany for determining the surface extension of Abu-Jir Fault Zone in Iraq: A new way for determining geometrical shapes of computational simulation models

Salih Muhammad Awadh *, Kamal Kareem Ali, Abbas Taha Alazzawi

Department of Earth Sciences, College of Science, University of Baghdad, Baghdad, Iraq

ARTICLE INFO

Article history:
Received 11 June 2012
Accepted 27 October 2012
Available online 3 November 2012

Keywords:
Geochemical exploration
Geobotany
Hydrocarbon survey
Fault zone
Spring water survey
Computational simulation model

ABSTRACT

The Abu-Jir Fault Zone (AJFZ) is a known fault zone and, as one of the typical structures in Iraq, extends NW-SE for a considerable distance on the western side of the Mesopotamian basin. The feature of this fault zone on the ground surface is mysterious and unclear. Surface extension evaluation of the fault zone requires the selection of valid parameters from among numerous geological factors. The present study focuses on the evidence of the existence of traces of the fault zone on the surface, such as springs, sites of hydrocarbon seepage, and geobotany, so as to employ them as tools in geochemical exploration for detecting the surface extension of the fault zone. For this purpose, direct and indirect geochemical methods including spring water survey (SWS), hydrocarbon accumulation and H2S gas survey (HAGS), and geobotanical survey (GS) were performed along the AJFZ. Hydrocarbon accumulations exist in many types of features. First, massive amounts of hydrocarbons ascend upward under high pressure piercing the gypsum of the Fatha Formation and exposed on the surface. Second, the hydrocarbon intrudes into the gypsum bed along the cleavage plane but is not exposed on the surface. Third, the light hydrocarbon ascends from the depth with the spring water and floats on the water surface. Anomaly in the distribution of hydrocarbon, total dissolved solid (TDS), H2S gas emission, abnormality in growth of palm trees (such as stem curvature and overturn, dwarfism), and the development of an isolated local aqueous environment around the springs along the AJFZ as well as computational simulation can be used to draw the geometrical shape of the fault zone on the surface. The surface extension of the AJFZ has been computed to be 467 km long with an average width of 48 km. This study has conclusively demonstrated the validity of the use of geochemical anomalies along with the computational simulation to estimate the dimensions of the fault zone.

1. Introduction

In general, hydrocarbons can accumulate beneath the surface at various depths. Under high pressure, hydrocarbons such as oil and gas squeeze and then move in response to the pressure toward areas of low pressure horizontally, obliquely, or vertically, according to the nature of the structure and permeability (API, 1996). Uncemented fault planes are the weak areas that act as suitable pathways for the migration of hydrocarbon-bearing fluids (Awadh et al., 2010). Fluids even remain in the hidden subsurface or rise up and flow on the surface. The appearance of hydrocarbons near the surface causes changes in soil chemistry and groundwater quality (Okieimen and Okieimen, 2005). The features of the plants change in response to the changes in water chemistry and soil. High salinity of hydrocarbon-bearing water may cause the toxic elements to concentrate resulting in the death of plants or the appearance of signs of illness in the stems, leaves, and fruits, or may permit the growth of only those plants that are salinity resistant such as tamarisk plant (Ethel tree). The Abu-Jir Fault Zone (AJFZ), first mentioned by Dunnington (1958), might have the character of a dextral wrench fault. The relatively high geothermal gradient in the upper Euphrates basin in the west of Iraq indicates that a fault plane is a pathway for the springs. Numerous geophysical survey methods have been developed to locate fault lines. Seismic (reflection or refraction), electrical, electromagnetic, and potential methods are typical examples of geophysical techniques. None of these methods can be said to be perfect as each has its own scope and limitations because of susceptible physical, electrical, and chemical properties of the Earth (Beck, 1981; Blyth and Fretis, 1984).

Oil seeps in the study area are located along the western boundary of the Mesopotamian basin. The seepages are situated on the N-S trending along the AJFZ. Bitumen lakes around 2 km in diameter are located at Abu-Jir, Ain Jabha, Ain Hit, and Ata'it (Aqrawi et al., 2010). Trapped oils of all the sources are preserved along the total petroleum system

* Corresponding author. Tel.: +964 7901214030.
E-mail address: salihauad2000@yahoo.com (S.M. Awadh).

0375-6742/$ – see front matter © 2012 Elsevier B.V. All rights reserved.
http://dx.doi.org/10.1016/j.gexplo.2012.10.011

between the highest regional seal of Middle Miocene-Lower Fars Anhydrite and the lowest seal of Upper Jurassic Gotnia Anhydrite with some other local seals of impermeable shales (Al-Ameri and Al-Obaydi, 2011). In the NW of the Zubair oil field, toward the Mesopotamian Basin boundary with the Zagros Fold Belt, the Zubair Formation has higher maturation in the Nahr Umr oil field. Therefore, 75% hydrocarbon generation of its efficiency has been obtained even as farther toward NE, 100% of its efficiency could be generated in the Majnoon oil field, which could be because of the increased thermal maturity closer to the suture of the Zagros Fold Belt (Al-Ameri et al., 2011).

On the other hand, many hitherto unsolvable geoscience problems have been solved using numerical methods and computational simulations (Schafer et al., 1998; Wang and Beckermann, 1993; Zhao et al., 1997). Nield and Bejan have summarized the early work carried out before 1992 on convective fluid flow in porous media in their book (Nield and Bejan, 1992). With the stimulus of exploring new mineral deposits and oil reservoirs, Zhao and his coworkers have carried out extensive and systematic research work to understand physical and chemical processes that control the formation of large mineral deposits and oil reservoirs within the upper crust of the Earth (Zhao et al., 2008a, 2009). The pioneering work of Zhao and his coworkers has remarkably enhanced the understanding of ore body formation and mineralization in hydrothermal systems, and is clearly marked by the following five milestones in the field of computational geosciences.

The first milestone work demonstrates that convective fluid flow can take place in the Earth's crust not only when the pore-fluid pressure is hydrostatic, but also when it is lithostatic. This resulted in a clear conclusion to the long-term debate in which it was commonly regarded that convective fluid flow cannot take place in the Earth's crust when the pore-fluid pressure is lithostatic (Zhao et al., 1999). This pioneering work was applied to understand the formation mechanisms of gold deposit in Yilgarn Craton, Western Australia (Sorjonen-Ward et al., 2002), Mt Isa lead-zinc deposit in Queensland, Australia (Ord et al., 2002), and copper-gold mineralization in the New Guinea (Gow et al., 2002).

The second milestone work demonstrates that convective fluid flow can take place in 3D fault zones (Zhao et al., 2003, 2004). This pioneering work was applied to understand the mineralization mechanisms not only in generic models (Alt-Epping and Zhao, 2010), but also in realistic geological models. In particular, based on this pioneering work, Zhao et al. (2008b) has first successfully answered the following scientific question: why are Au deposits distributed with equal distance in the Bardoc fault of the Yilgarn Craton, Western Australia?

The third milestone work demonstrates fluid focusing and mixing behaviors within and around large cracks, fractures, and fault zones (Zhao et al., 2006, 2007). Through this pioneering work, it is concluded, from the theoretical point of view, that fluid pressure is hydrostatic or very close to hydrostatic within large cracks, fractures and fault zones (Zhao et al., 2008a). As the flow rate plays an important role in transporting ore-forming minerals and is strongly dependent on the permeability of a porous medium through Darcy's law (Zhao et al., 2010), the fourth milestone work considers the effect of the temperature-induced porosity and permeability variation on fluid flow in ore-forming systems including fault zones (Zhao et al., 2008a). The main conclusion drawn from this pioneering work demonstrates that the effect of the temperature-induced porosity and permeability variation on fluid flow is significant in soft rocks and fault zones.

The fifth milestone work demonstrates the effect of the mineral-dissolution-induced porosity and permeability evolution on the flow patterns in ore-forming systems (Zhao et al., 2008c). The Zhao number is, for the first time, proposed to represent the hydrodynamic characteristics of a mineralization system involving chemical dissolutions (Zhao et al., 2009). Using the Zhao number and its critical value, it is possible to judge whether an ore-forming system is in a stable or in an unstable state. In the latter state, fingerlike flow channels can be generated so that fluid focusing can take place in these channels.

The pioneering work of Zhao and his coworkers has resulted in the establishment of the emerging computational geoscience discipline (Schmidt et al., 2010). As computational simulation is a core element of computational geoscience, the pioneering work of Zhao and his coworkers has been also widely applied to solve many geoscience problems, not only in Australia (Gessner et al., 2009; Hobbs et al., 2000; Kühn et al., 2006; Schaubs and Zhao, 2002; Yang et al., 2006, 2010; Zhang et al., 2003, 2008, 2010) and China (Ju et al., 2011; Lin et al., 2006, 2008, 2009; Liu et al., 2005, 2008, 2010a, 2010b, 2011; Yan et al., 2003; Zhang et al., 2011), but also in the elsewhere of the world (Fu et al., 2010; Harcouët-Menou et al., 2009; Magri et al., 2010; Wang et al., 2010; Xing et al., 2008).

In order to provide realistic rendering of fault zones in reservoir models utilizing stochastic methods, quantification of some basic fault attributes e.g. distributions of fault length and thickness, fault aspect ratio (fault length divided by height), fault orientation, density and spacing of fault-related structures in the damage zone are required. In practice, 3D models are generated based on frequency distributions of fault attributes deduced from 2D maps and sections or 1D logs (Harris et al., 2003). Although a number of review papers have previously addressed fault scaling laws (Bonnet et al., 2001; Childs et al., 2009; Harris et al., 2003; Kim and Sanderson, 2005; Odling, 1997; Schultz and Siddharthan, 2005; Schultz et al., 2008; Sibson, 1989) and the observed scatter in the data, none of them covers all aspects of this important topic.

For the purpose of effectively using the above-mentioned contemporary knowledge and computational methods to solve complicated geoscience problems involving fault zones (Zhao et al., 2009), it is necessary to determine the geometrical shapes and related parameters of the fault zones as accurately as possible. Although some geological and geophysical methods are available, it is also desirable to develop some geochemical tools to determine the geometrical shapes and related parameters of the fault zones. For this purpose, the present study discusses the relationship among the spring water, hydrocarbon seepages, and geobotanical features and their anomalies along the AJFZ using computational simulation of the geometrical shape of the fault zone in an attempt to determine its surface boundaries (length and width), so that it can be drawn on the map as a zone, rather than as a line.

2. Location of the study area and geological setting

The study area is located in the extreme east of the Western Iraqi Desert. It represents the AJFZ that is a long strip along the western border of the Mesopotamian basin (Fig. 1) and is separated from the Salman Zone (in the Widian Basin) that is considered as a part of the Stable Zone, according to the Iraqi tectonic divisions. The western part of Iraq is divided tectonically into basins and uplifts that form many gravitational faults and grabens (Pollastro et al., 1999). The Widian basin is a graben structure on the western side of the AJFZ. The uplifts and subsided sites have formed many structural closures that may form traps for the hydrocarbon accumulations. Many lineaments, structures, and faults have been identified in Iraq and described in detail (Jassim and Buday, 2006). The dominant orientation trends of the palaeostructures in Iraq are NW-SE, NE-SW, W-E, and N-S. These structural orientations were first noticed by Henson (1950). Iraq is a part of the Arabian shelf, which is tecto-physographically divided into the Unstable Shelf in the northern Iraq and the Stable Shelf that represents the unfolded area in the remaining parts of Iraq. The tectonic divisions of Iraq can be outlined as the Thrust Zone, High Folded Zone, and Low Folded Zone (Mosul-Butma Subzone and Kirkuk-Hamrin Subzone). They are the major features of the northern part of Iraq, which represent the Unstable Shelf of the Arabian Shield in Iraq (Fig. 1). The Stable Shelf, which comprises the rest of the tectonic features of Iraq, was formed by the Mesopotamian Basin, Salman Zone, and Rutba-Jazera Subzone. The AJFZ separates between the Mesopotamia Basin and the Salman Zone (in the Widian basin) (Fig. 1). Groundwater recharge, transmission,

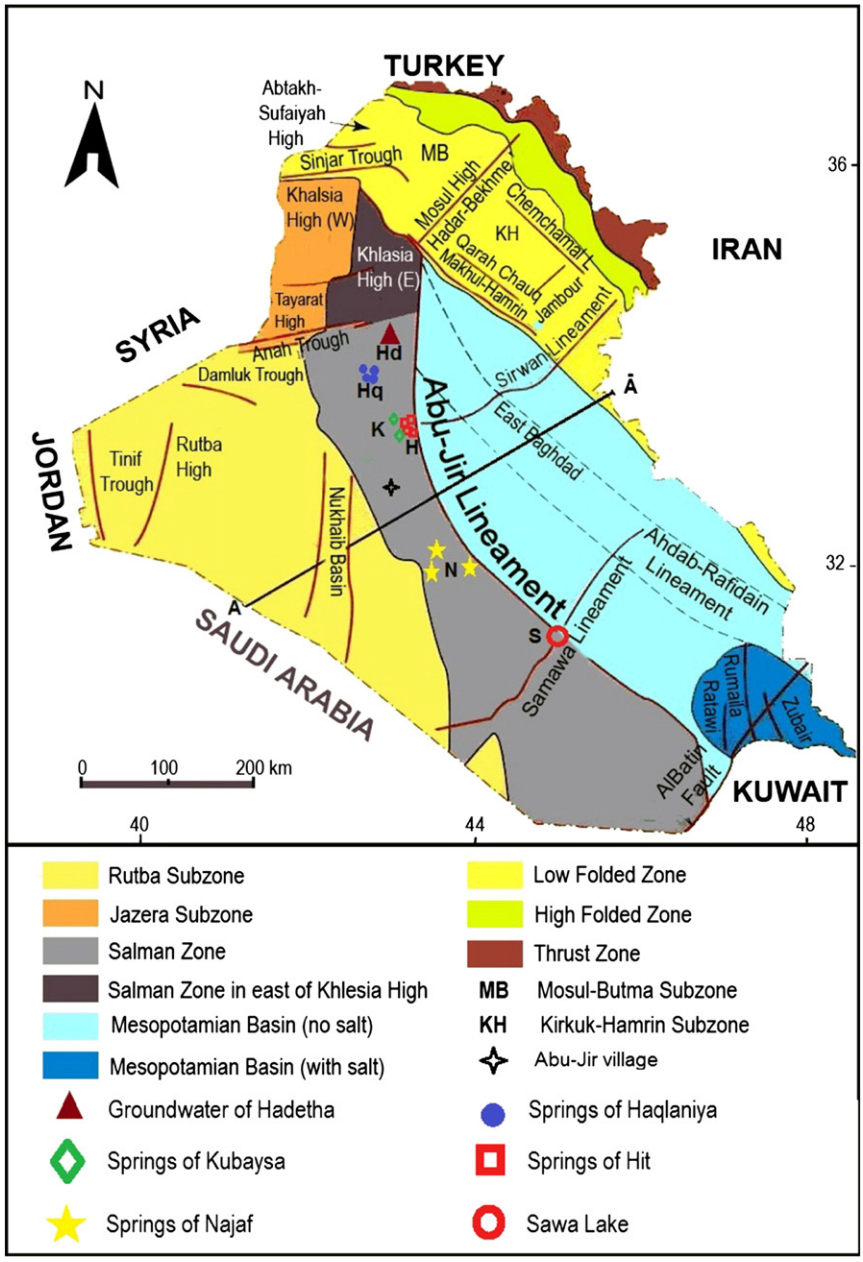

Fig. 1. Simplified tectonic map shows the sampling sites in the study area.

and discharge of a basin are controlled by the basin geomorphology, geology, and structural patterns of a region. The AJFZ crosscuts the Paleozoic, Mesozoic, and Cenozoic units (Fig. 2). This figure illustrates that the seismic profile shows the AJFZ across the Mesozoic and Paleozoic sequences through profile A-Á seen in Fig. 1. The Khabour Formation (Late Ordovician) is made up of sandstone and shale bed in well Akkas-1 (2325–4228 m, greater than 2103 m thick) and Khlessia-1 (2544–3792 m, greater than 1248 m thick) (Aqrawi et al., 2010) in the Western Desert of Iraq. This formation in its lower part can be correlated with the Hanadir Member of the Qasim Formation in the NE Nafud Basin in northern Saudia Arabia (Al-Hajri and Owens, 2000), which has a total organic carbon (TOC) content of 1.13 (Schlumberger, 1991) and also correlated with the shales in the Hiswah Formation at the Risha gasfield in Jordan (Powell, 1989a, 1989b), where it has 2% TOC and contains Type II kerogen (Beydoun et al., 1994). The Chia Zairi Formation (Late Paleozoic) is composed of limestone and some dolomite and chert. It contains in the lower unit thin bedded organic detrital limestones and black shale (Buday, 1980). The Kurra Chine Formation (Upper Triassic) is composed of dark brown to black limestone, dolomite, and some papery shale (Bellen et al., 1959). It is deposited in lagoons, sometimes with euxinic influence. The Alan Formation is the supermost formation of the Liassic in the western part of the Unstable Shelf and on the Stable Shelf in Iraq (Buday, 1980). It is composed of anhydrite with subordinate pseudoolitic limestones. The Gotnia formation in central Iraq consists predominantly of massive anhydrite with thin interbeds of brown calcareous shale (Dunnington et al., 1959), whereas in southern Iraq, it contains chalky limestone (Roychoughury and Handoo, 1980). It has a thickness of about 193m in central Iraq (Aqrawi et al., 2010). The Gotnai Formation would have created conditions suitable for the deposition of organic-rich source rocks (Aqrawi et al., 2010). Alsharhan and Kendall (1986) and Al-Sakini (1992) have suggested that euxinic conditions in this basin resulted in the deposition of black, organic-rich shale and limestones with source rock potential. The kerogen type in the Gotnia Formation was mostly amorphous and of marine

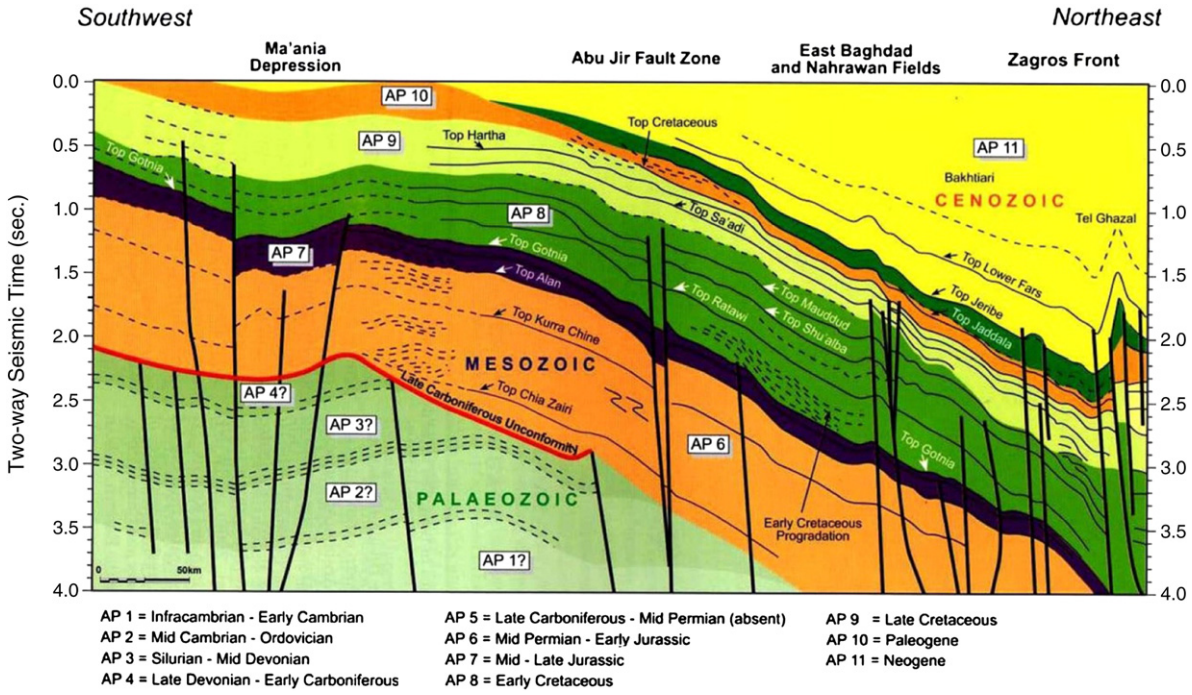

Fig. 2. Regional-scale seismic profile shows the Abu-Jir fault Zone across the Mesozoic and Paleozoic sequences (after Mohammad, 2006).

origin (Aqrawi et al., 2010). The AJFZ crosscuts the Paleozoic and Mesozoic sequences (Fig. 2). The other formations that are crosscut by the AJFZ are the Ratawi Formation, Shu'aiba Formation, Mauddud Formation, Saadi Formation, and Hartha Formation.

3. Hydrological system

The Anah and Euhrates Formations are the major aquifers in the northern part of the AJFZ (near Hadetha, Haqlaniya, Hit, and Kubaysa), whereas the Dammam and Euphrates Formation form the hydrological system at the southern part of the AJFZ (near Najaf and Samawa). The Umm Er Radhuma Formation is the main and deepest aquifer in the Western Desert. The average thickness of the Euphrates Formation is about 80 m, whereas the Dammam ranges from 70 to 200 m. The dip of layers in the Western Desert is generally eastward. Accordingly, the main flow of groundwater is eastward. The Dammam Formation consists of a deep confined aquifer and a shallow confined aquifer. There is a partial connection between these aquifers, leading to the water flow from the deep aquifer upward to the shallow aquifer. The water chemistry of these aquifers is almost similar. There are seasonal exchangeable relationships between the aquifers and the Euphrates River, depending on the water level.

4. Materials and methods

4.1. Sampling and analytical methods of water

Ground water, spring water, and lake water were investigated on six sites: north of Hadetha (one well), Haqlaniya (four spring waters), Hit (four spring waters), Kubaysa ((two spring waters), Najaf (three spring waters), and the site represented by the Sawa lake. Field parameters such as total dissolved solid (TDS), electrical conductivity (EC), pH, and temperature were measured onsite using a portable multimeter device. Water samples collected from the well and springs were transported to the laboratory the same day and filtered using a 0.45 μm millipore filter paper. The samples were acidified to pH < 2 with several drops of ultrapure HCl in the laboratory and then refrigerated. Samples were analyzed for major ions, using the standard methods (APHA, 1995). Samples were analyzed for sulfate and nitrate, using UV/visible spectrophotometer; for sodium and potassium using flame photometer; and for calcium, magnesium, chloride, and alkalinity (HCO3 + CO3) using the titration method. Overall, measurement reproducibility and precision for each analysis were less than 2%. The analytical precision for the total measurements of ions was checked again by calculating the ionic balance errors and was generally within ±5%. The results of water chemistry are listed in Table 1. The global positioning system (GPS) from e-Trex, German, was used to determine the coordinates of all sites (Table 2).

4.2. Sampling of hydrocarbons and gypsum

Solid hydrocarbons from the masses seeped on surface were sampled at the Hit, Hadetha, and Najaf areas, whereas liquid hydrocarbons were sampled from those floated on the surface of the spring water at the Hit area. Outcrops of hydrocarbons-bearing gypsum were sampled. Many thin sections were prepared in the workshop at the Department of Earth Sciences, College of Science, University of Baghdad. A polarized microscope was used for the purpose of clarifying the relationship between the hydrocarbon and gypsum.

4.3. Determination of dissolved H2S gas

The H2S dissolved gas was determined in the field using the procedure of 4 ml of 20% of (CH3COO)2Zn and 1 ml of 1N of NaOH, which are transferred into the volumetric flask of 100 ml. The flask was subsequently filled with sample water and sealed well. Here the sample becomes foggy with a white suspension of zinc sulfide. The zinc sulfide precipitates according to the equation given below:

$$(CH_3COO)_2Zn + 2NaOH + H_2S = Zns + 2CH_3COONa + 2H_2O$$

The S2- concentration was computed using the mole concentrations of zinc, sulfur, and hydrogen.

Table 1
The hydrochemical parameters of the water in the study area.

Site name	Sampling media	Sample no.	Na epm	SO4 epm	Cl epm	rNa/rCl	(rNa-rCl)/rSO4	rSO4/rCl	TDS ppm	Origin
Hadetha	Well	1Hd	11.4	6.3	52.5	0.22	−6.5	0.12	12700	Marine
Hqlaniyia	Spring	1Hq	10.9	5.4	45.7	0.24	−6.4	0.118	2820	Marine
	Spring	2Hq	10.0	4.4	46.5	0.215	−0.56	0.090	2940	
	Spring	3Hq	10.2	4.2	47.1	0.216	−1.01	0.089	2930	
	Spring	4Hq	10.4	8.1	54.3	0.19	−5.4	0.149	3470	
Hit	Spring	1H	12.6	4.4	102	0.12	−19.9	0.123	5600	Marine
	Spring	2H	8.70	4.7	82.8	0.10	−15.8	0.105	4760	
	Spring	3H	11.7	5.0	88.6	0.13	−15.4	0.132	4890	
	Spring	4H	12.6	5.6	91.4	0.14	−14.2	0.137	5070	
Kubayssa	Spring	1K	11.3	10.4	57.4	0.19	−4.43	0.196	3770	Marine
	Spring	2K	10.9	14.6	85.7	0.13	−5.13	0.127	5350	
Najaf	Spring	1N	13.0	6.5	71.4	0.18	−9.04	0.181	4100	Marine
	Spring	2N	11.7	6.0	73.1	0.16	−10.24	0.160	4200	
	Spring	3N	11.3	5.6	68.6	0.164	−10.2	0.164	4000	
Samawa	Lake	1S	260	187	264	0.98	−0.02	0.513	27500	Marine

4.4. Scaling of the fault zone

Knowledge of the spatial distribution of different fault attributes such as length, displacement, and thickness and the relations between them has been the focus of considerable attention over the past decades among geoscientists (Childs et al., 2009; Cowie et al., 1994). It is very necessary to determine the geometrical shape of the fault zone and the topography of the surrounding land. A computational simulation was conducted to determine the geometrical shapes of the AJFZ. To achieve this purpose, the Surfer software program, version 9 was used. Data of the longitudes, latitudes, and elevations of a rectangular area (200×500 km) were input to the computer. Then a contour map and a wire frame map were drawn (Fig. 3). For determining the length and width of the AJFZ, the groundwater flow rate, permeability or hydraulic conductivity, cross-sectional area (the saturated thickness of a confined aquifer multiplied by the aquifer width), and the piezometric water elevation were measured. Then, by using Darcy's law, the distance between the springs was determined. This distance can be further used to determine the length and width of the Fault zone.

5. Results and discussion

5.1. Hydrocarbon accumulation and H2S gas survey (HAGS)

Oil and gas reservoirs can leak. As a result, large quantities of oil and gas from these reservoirs may reach the surface to form seeps. Within the water spring column, the upward seeping gas produces bubbles that can be detected and easily noticed by the eye forming subsurface chimneys along which oil and gas migrate to the surface. The hydrocarbon accumulations are observed on the surface and subsurface. The hydrocarbon seeps onto the surface at the Hit and Al-Najaf areas (Fig. 4), whereas it was accumulated under the subsurface in Hadetha (Fig. 5) and Hit. The migration of hydrocarbons may be in horizontal, oblique, and vertical movements. Hydrocarbons migrated from the source rock upward to cross many formations and then interfered with the gypsum of the Fatha Formation. Accordingly, part of the hydrocarbon reaches the surface. Petrographic study of thin sections revealed that the hydrocarbons moved under high stress, piercing the cleavage plane of gypsum and its fractures (Fig. 6). Some gypsum grains change into anhydrite, resulting in the release of 2H2O. Hydrocarbon microseepage gives rise to expressions at the Earth surface in the form of: (1) detectable trace concentrations of gasses (mainly ethane and methane), (2) mineral alteration of soils, and (3) anomalous spectral response in vegetation (Van der Meer et al., 2000).

The direct detection is defined as the detection of either oil pools or mineral alteration related to seepages. Methods of indirect detection focus on secondary effects resulting from seeping light hydrocarbons to the surface. These relate to changes in the vegetation. Seeps occur predominantly in areas that are tectonically active (Van der Meer et al., 2000). The amount of seepage potentially is related to the pressure in the reservoir, which is related to hydrostatic pressure and changes in lithospheric stress. Thus in natural seepages, a relation between the amount of seeping gas and stress could be envisaged. Bubbles of H2S gas can be seen in most of the springs; they are clearly visible in both Hit and Kubaysa, whereas it is less pronounced in the springs of Haqlaniya, Najaf, and Sawa. This reflects the amount of gas liberated, which indicates the relative position of the spring moving within the faulted zone. The geochemical seepage model indicates that bacterial degradations of light hydrocarbons seeped upward from traps to create a reduction zone along the fault planes of the AJFZ.

Table 2
Coordination of sampling location in the study area.

Site name	Sampling media	Sample no.	Coordination		
			Latitude	Longitude	Elevation (m)
Hadetha	Well	1Hd	34 15 7.5	42 34 11.88	216
Hqlaniyia	Spring	1Hq	34 05 24.71	42 21 59.81	90
	Spring	2Hq	34 05 24.62	42 21 59.83	88
	Spring	3Hq	34 05 24.50	42 21 59.85	90
	Spring	4Hq	34 05 24.55	42 21 59.84	90
Hit	Spring	1H	42 44 18.3	33 39 53.5	85
	Spring	2H	42 48 51.9	33 38 20.9	60
	Spring	3H	42 49 51.4	33 37 48.8	56
	Spring	4H	42 50 10.3	33 38 19.8	50
Kubayssa	Spring	1K	42 35 36.71	33 35 53.4	114
	Spring	2K	42 36 47.5	33 34 6.7 1	120
Najaf	Spring	1N	43 13 45.0	31 55 37.3	13
	Spring	2N	44 05 45.0	31 37 32.4	57
	Spring	3N	44 05 26.7	31 56 24.9	42
Samawa	Lake	1S	45 01 38.12	31 17 49.68	17

5.2. Spring water survey (SWS)

Thirteen spring waters as well as ground water and the lake were surveyed along the AJFZ. These waters distribute along a long curved track of the fault. They contain a variety of anomalies of hydrocarbons. Hydrocarbons mixed with water were perfectly noticed within the groundwater at Hadetha and Hit. The low viscosity is characterized from the hydrocarbon of Hadetha, whereas high viscous hydrocarbon is detected at Hit area. As all hydrocarbons are lighter than water, they float on the surface of the water (Fig. 7). H2S gas escaping from spring water can be ignited with a flame of fire to a height of

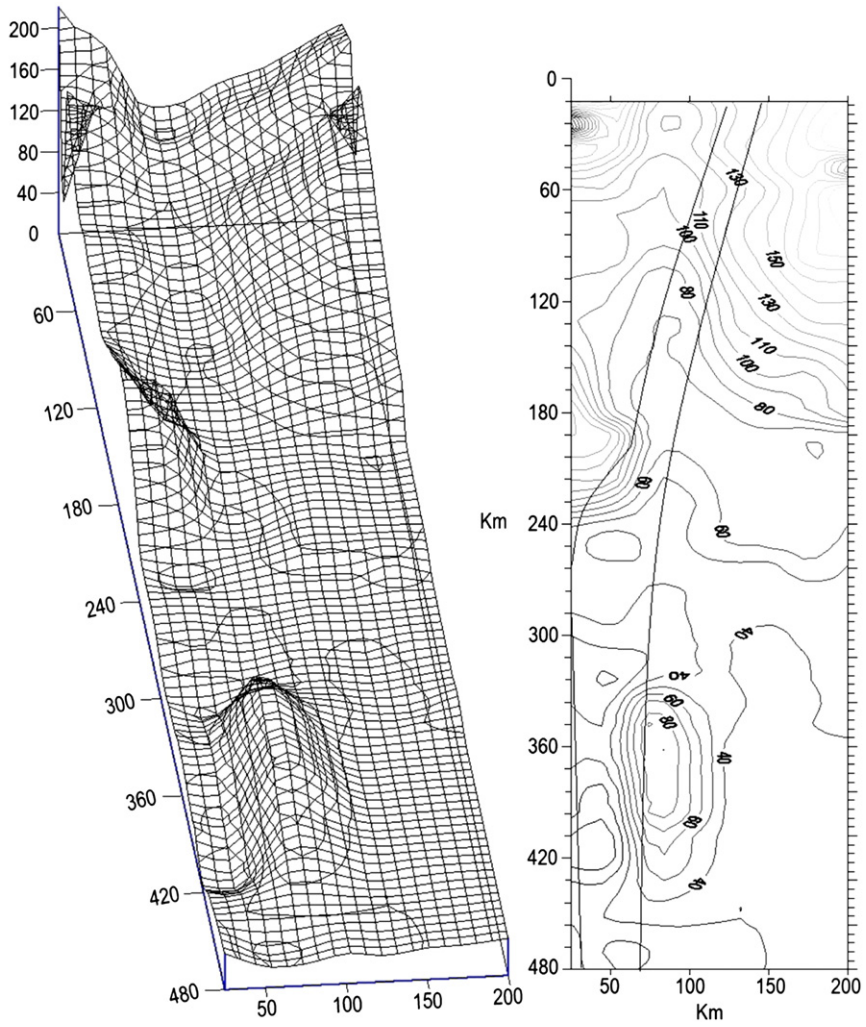

Fig. 3. Flat contour map and wire frame map simulate the geometrical shape of the AJFZ on the surface.

about 1 m. This can clearly be seen when local people set the H2S bubbles on fire (Fig. 8).

The hydrochemical results are listed in Table 1. The available information indicates great similarities in water chemistry among the study areas. Minor differences in the chemistry of spring water can be attributed to the various dilution processes, including the aquifer recharge from the Euphrates River, the amount of precipitation in each area, the partial mixing between the aquifers of the hydrological system, and the connection with fracture zones along the AJFZ.

All spring waters originate from the deep source of marine origin (Fig. 9). Water chemistry revealed the relative similarity between the springs of Kubaysa and Haqlaniya, where they partially approach

Fig. 4. Hydrocarbon seepage on the surface. a, mass of hydrocarbon-bearing gypsum at Hit area; b, hydrocarbon accumulations covered by thin siol layer at Najaf area.

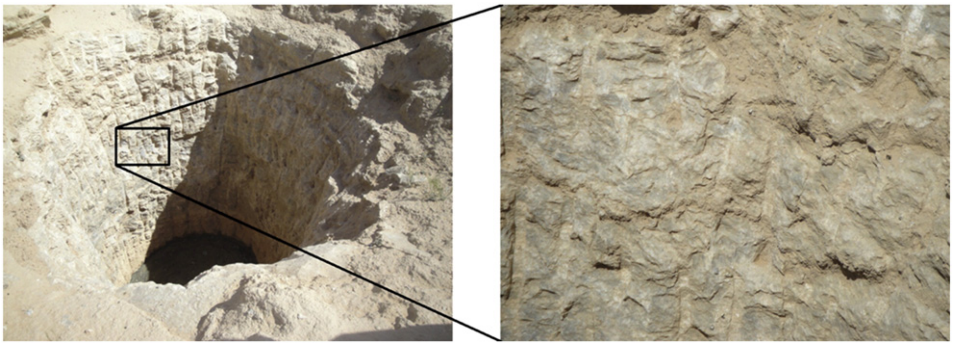

Fig. 5. Hand dug well with 4 m diameter displays the subsurface pattern of hydrocarbon-bearing gypsum.

the marine origin with high dilution. The springs of the Hit area are closer to the marine nature at the specific location on the main fault plane of the AJFZ (Fig. 10). The springs of Najaf are characterized by the water chemistry almost similar to the groundwater of Haditha. Haditha and Najaf are located far apart as the terminal end of the fault approximately. The total dissolved solid (TDS) is generally high, especially in the Sawa lake (1S) and the water well of Hadetha (1Hd), whereas it decreases relatively in the spring water of Haqlaniys, Hit, and Najaf because of the dilution caused by the river and meteoric water (Fig. 11). The extreme value of TDS in the Sawa Lake was caused by evaporation.

5.3. Geobotanical survey (GS)

The hydrocarbon effects may often be reflected in the health and type of vegetation over the seep (Matthews et al., 1984; Patton and Manwaring, 1984; Weismann, 1980). The health of palm trees in the investigated areas appears to be affected by the same level of similar factors. The dwarfism of palms and irregularity of stem in restricted areas are the evidence of falling under the influence of nutrients coming through the fault plane, where the hydrocarbon seepage was found to influence the soil and the vegetation around the seeps. The most important changes in the soil are microbiological changes, formation of new minerals such as calcite, pyrite, and uranium, bleaching of red beds, electrochemical changes, and radiation anomalies (Schumacher, 1996; Tedesco, 1995). Vegetation growing near the hydrocarbon seeps can have changes in the geobotany, biochemistry, and reflectance (Bammel and Birnie, 1994). Studies on vegetation growing near leaking gas pipelines revealed changes in geobotany and reflectance (Pysek and Pysek, 1989; Smith et al., 2000).

The changes in geobotanical features, such as the creeping stems of palm trees with the curvature (Fig. 12) and sometime stem overturn in the areas of Hit, Kubaysa, and Najaf, indicate hydrocarbon seepage and reflect the track of the fault on the surface. The similarity of the external features of the palms refers to the similarity of hydrocarbon

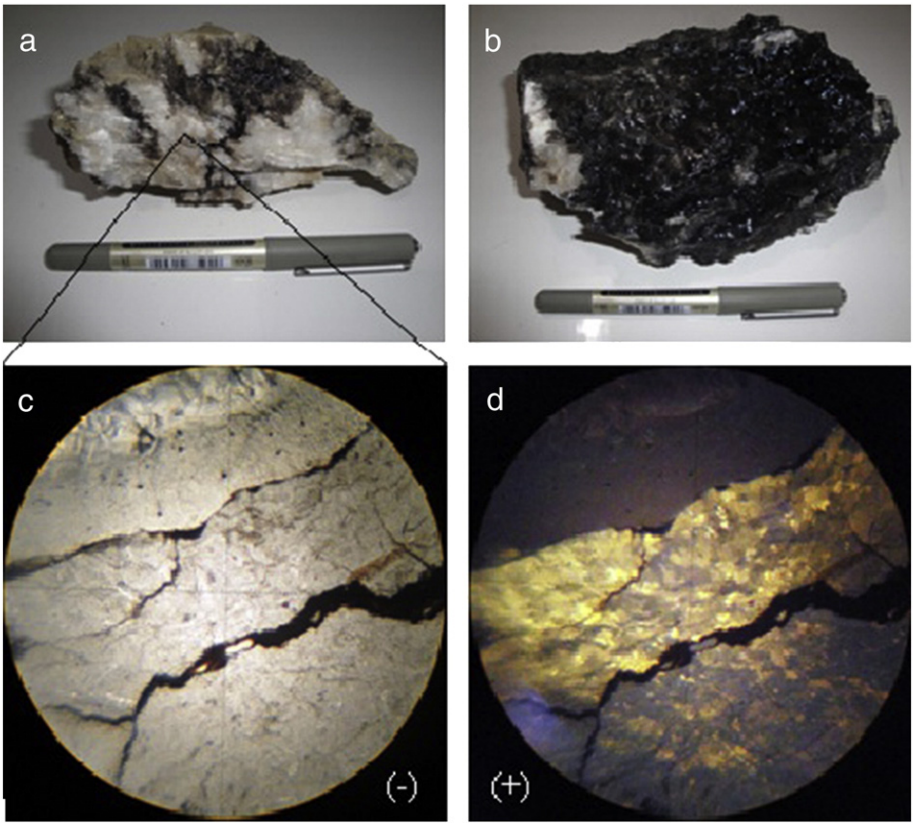

Fig. 6. The hydrocarbon-bearing gypsum collected from the outcrops of Fatha Formation at Hit area; a and b, Hand specimen samples; c and d, micrographs display how the hydrocarbon (black) penetrates the cleavage planes and fractures of gypsum.

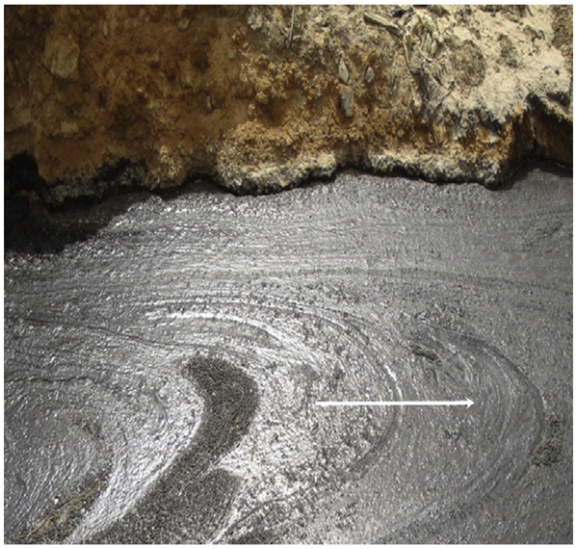

Fig. 7. Hydrocarbon floats on the surface of spring water at Hit area, arrow points the flow direction.

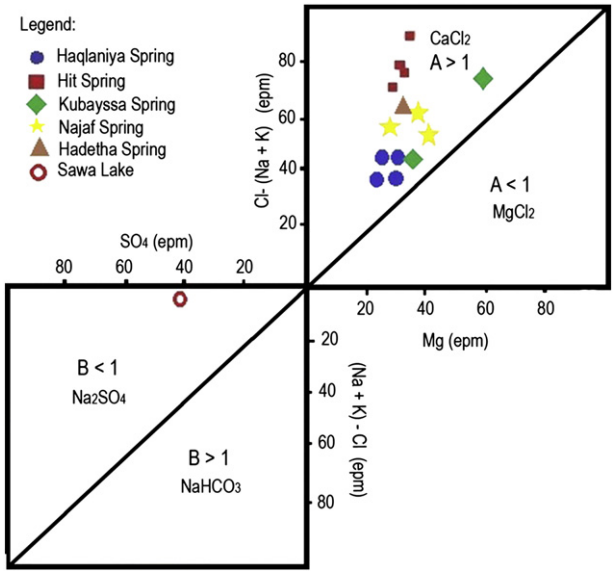

Fig. 9. Sulin classification illustrates the type of water.

origin as well. The Halophyte flora grown locally around the spring environment also was considered as a geobotanical indicator of the source. Halophyte floras are the characteristic of saline environments (Colin, 2007). Halocnemum strobilaceum is a dominant species in water containing 6300–9500 ppm Cl (Habib et al., 1971). Chloride is below this range, but, in general, it tends to be high. The GS revealed a presence of relationship among springs, hydrocarbon seeps, and vegetation, which is considered as the fingerprint of the surface extensions of the AJFZ.

5.4. Surface extension of the AJFZ

The surface feature of faults in the flatland tends to be uncertain because they are hidden under the surface. These faults can be detected through their fingerprints.

Structural controls on mineralization in the upper crust of the Earth have been an important topic for many years (Cox, 1999; Hodgson, 1989; Leach and Rowan, 1986; Matthai, 2003; Norton and Knight, 1977; Oliver, 1995; Phillips, 1972; Valenta et al., 1994; Zhao et al., 2012). The computational simulations provide a new way to deal with the many geosciences problems (Zhao et al., 2009). Crystal rock can be treated as a porous medium, in which porosity is used to describe the pore volume per unit volume rock. In such a porous medium, fluid can flow in the channels that are formed by the connecting pores and fractures (Lin et al., 2003). The flow-focusing factor is defined as the ratio of the maximum fluid flow velocity in the fault to the inflow velocity within the surrounding rocks. Fluids flow in fluid-saturated porous rocks is commonly described using Darcy's law (Zhao et al., 2008a). Darcy's law is the basic equation that describes fluid flow through porous media. It is also known that the Darcy flux, which is defined as the flow per unit cross-sectional area of the porous medium, can be defined by the equation below:

$$Q = KA\frac{H1-H2}{L} \quad (1)$$

where Q is the groundwater flow rate, K is the hydraulic conductivity, A is the cross-sectional area (the saturated thickness of a confined aquifer multiplied by the aquifer width), H1–H2 is the piezometric water elevation difference, and L is the distance between springs.

This study estimated that the average of groundwater flow rates (Q) from measurements within an aquifer is 0.72 l/s. An estimation of the hydraulic conductivity (K), which was made from knowledge of the geologic material and aquifer hydraulic tests, is 1.4×10^{-4} m/s. The cross-sectional area (A) is the saturated thickness of a confined aquifer multiplied by the aquifer width. The piezometric water elevation difference (H1–H2) can be measured from the measurement installation of springs. The distance between springs (L) can be computed by using Darcy's law, which can be used to find the maximum length (L) between springs along the AJFZ. The piezometric water elevation difference (H1–H2) between the Hadetha in the north and the Samwa in the south is 40 m. By using Darcy's Law, we find that the length (L) is equal to 467 km, which represents the length of the fault zone in the study area (Fig. 3). For the purpose of calculating the average width of the fault zone, three sites in the study area were selected, the northern part, central part, and southern part. Accordingly, the piezometric water elevation differences (H1–H2) in these parts were determined to be 0.24 m, 0.58 m, and 0.41 m, respectively. It was computed between the two extreme springs perpendicular to the fault zone extension in each part. Thus, by using Darcy's Law, we found that the width of the AJFZ is equal to 28, 67.6, and 47.8 km, respectively. This means that the average width of the AJFZ is 48 km. The surface geometrical shape of the AJFZ is illustrated in Fig. 3. To ensure the accuracy of the results

Fig. 8. Fire flam at the surface of spring water yielded from the ignition of H2S.

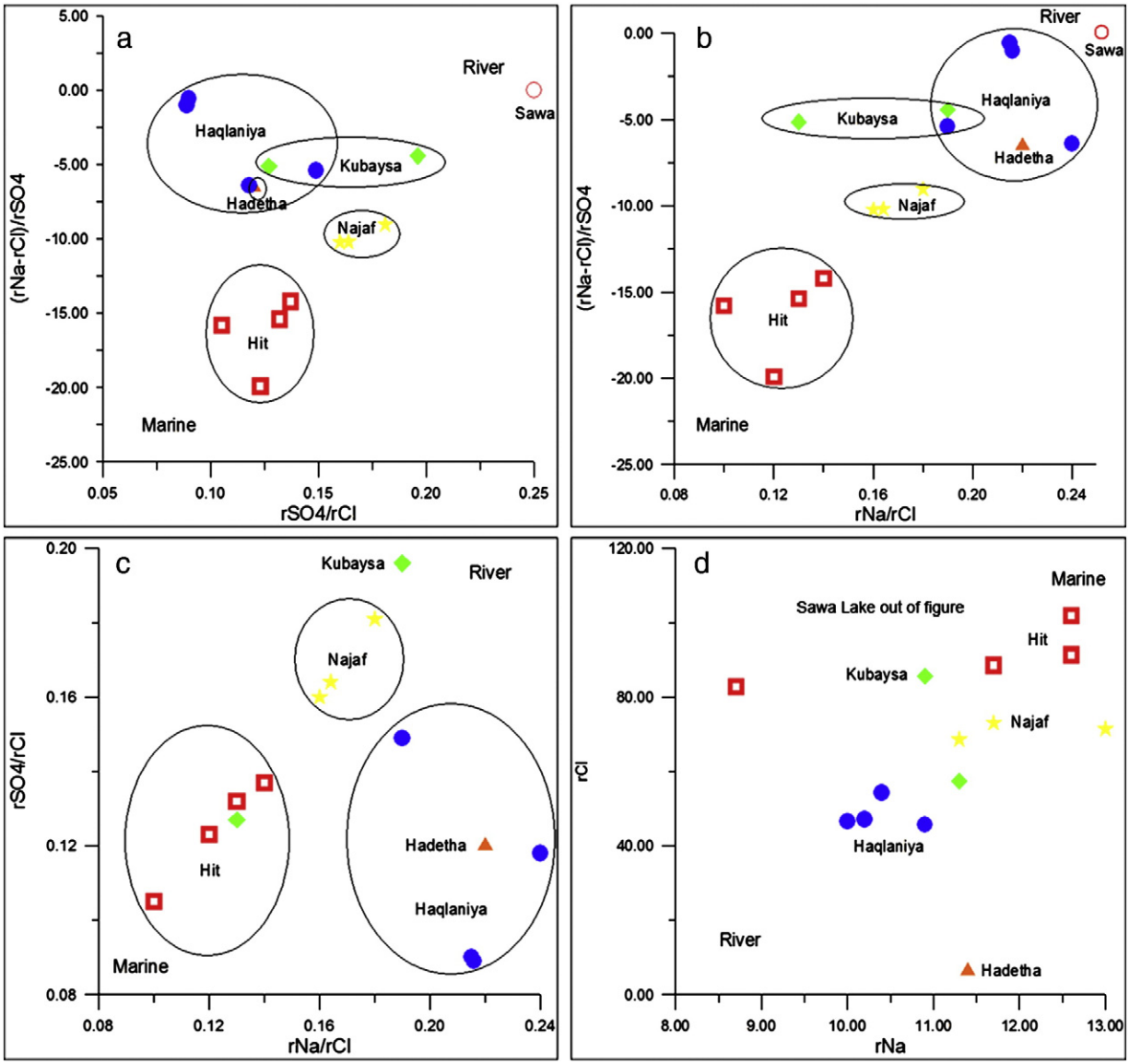

Fig. 10. Functions of hydrochemical ratios of 14 springs collected from five areas along the AJFZ as well as the Sawa Lake.

we have mathematically obtained, the fault dimensions were calculated again based on the distribution feature of springs. The results were similar and satisfactory. The idea and procedure can be explained here. Spring water survey, HAGS and GS have recorded clear anomalies that are deviated from the background. Springs, hydrocarbon seepages, and the geobotanical features can be used to draw a map of the fault zone on the surface. Through follow-up anomalies resulting from different types of geochemical surveys, the detection of the fault zone becomes possible. Accordingly, the surface extension of the AJFZ was mapped and fixed on an aerial map (Fig. 13). The process of determining the width of the fault zone can be summarized by plotting all anomalies resulting from SWS, HAGS, and GS on the aerial map based on the GPS coordination. Thereafter, three widths of the AJFZ were computed, depending on the scale of the map. The width of the AJFZ in its north part, middle part, and south part was computed to be 27.5, 67.5, and 47.5 km, respectively. The average width is 47.5 km. Although the length of the AJFZ has been determined to extend to the south of Iraq by the previous studies, the present study demonstrated that the proven length of the AJFZ beneath the geochemical anomalies in the study area is 464 km. The result of this study allows us to map the AJFZ as a zone, rather than just as a line.

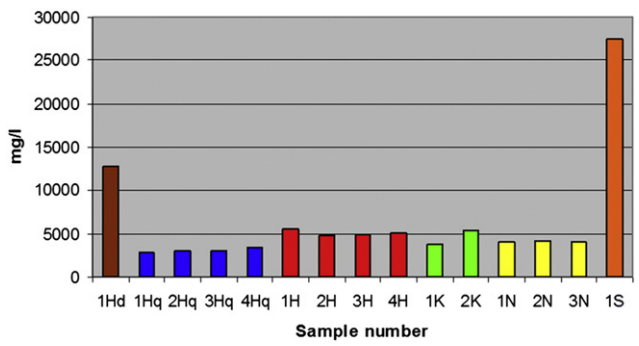

Fig. 11. Total dissolved solid in the well, spring waters and Sawa Lake.

6. Discussion and conclusions

To effectively use contemporary knowledge and computational methods to solve complicated geoscience problems involving fault zones (Zhao et al., 2008a, 2009), it is necessary to determine the geometrical shapes and related parameters of the fault zones as accurately as possible. Although some geological and geophysical methods are

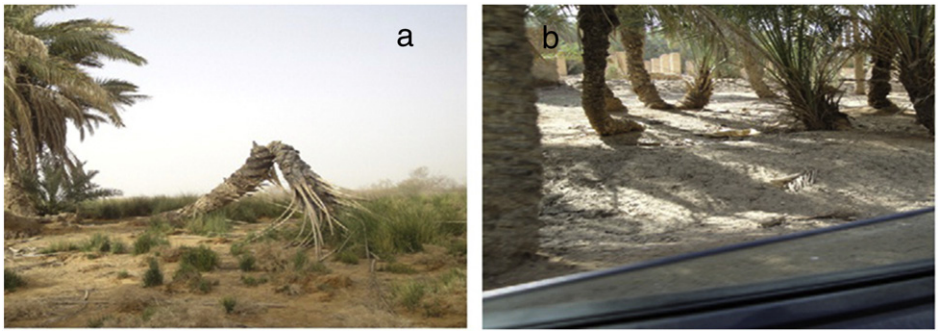

Fig. 12. Creep and curvature of the palm trees; a: at the Najaf, while b at the Kubaysa.

available, it is also desirable to develop some geochemical tools to determine the geometrical shapes and related parameters of the fault zones. For this reason, the relationship among spring water, hydrocarbon seepages, geobotany and their anomalies along the AJFZ has been established to determine the surface boundaries (length and width) of this fault zone.

Faults play an intricate role in hydrocarbon migration and accumulation as they can serve either as a conduit or a seal (Zhang et al., 2011). The presence of numerous amounts of bitumen, H2S gas, and spring water seepage within the AJFZ provide information on preferential pathways that the leakage has followed (Awadh et al., 2010). The hydrocarbon seepage directly above oil and gas reservoirs shows that the hydrocarbons seep (nearly) vertically to the surface (Tedesco, 1995). Seepages might originate from great depths beneath the AJFZ or from the reservoir. The oil migrated to the low pressure area, which is connected with the AJFZ. The subsurface strata near the Haditha city could have oil and gas generated from the Upper Jurassic Sulaiy Formation as a source and accumulated within a pay of petroleum system of the Cretaceous to Tertiary ages. The seep oil in this area is of the same type as the East Baghdad oil field of the Mesopotamian Basin to the east and of a type different from the Akkas field of the Wedian Basin to the West (Al-Rawi et al., under review). The mechanism of transportation can be subdivided into two categories, effusion and diffusion, which are principal mechanisms that lead to the gas seepage. Bacterial degradation is an effective process to generate H2S. The dissolved H2S gas in the groundwater as a result of hydrodynamic and chemical potential has been observed through seemingly impermeable capping of the Fatha gypsum. This form of migration contributed to the microseeps. Pressure-gradient driven fluid flow can cause mass transport in the fluid-saturated porous rock. Fluid flow induced by the uneven surface topography of a basin and the flow of fluids squeezed out of a sedimentary basin by crustal deformation are typical examples of fluid pressure-gradient driven flow (Bethke, 1985; Oliver, 1986). Several springs particularly at the Hit area pointed to a network of interconnected fractures. The fault planes serve as the channels that allow microbubbles to migrate between the hydrocarbon reservoirs and the surface. Because of the lack of clarity of dislocations of the fault at the surface, the AJFZ can be best understood by tracking the spring water sites that draw the lateral and longitudinal fault extension. The spring waters demonstrate that the water genesis is of marine origin of deep source with different rates of partial mixing with the meteoric water. The general direction of the groundwater movement in the Western Desert of Iraq is eastwardly. Accordingly, groundwater crosses the fault plane, and then ascends upward to the surface as springs. The changes in geobotanical features such as stem curvature and stem overturn of palm trees within the AJFZ are also evidences of hydrocarbon microseepage, which defines the fault line on the surface. The local salty aquatic environments near the springs indicate the same origin of spring water, which confirms that all aquifers have been cut by the fault planes of the AJFZ. According to the spread of hydrocarbon

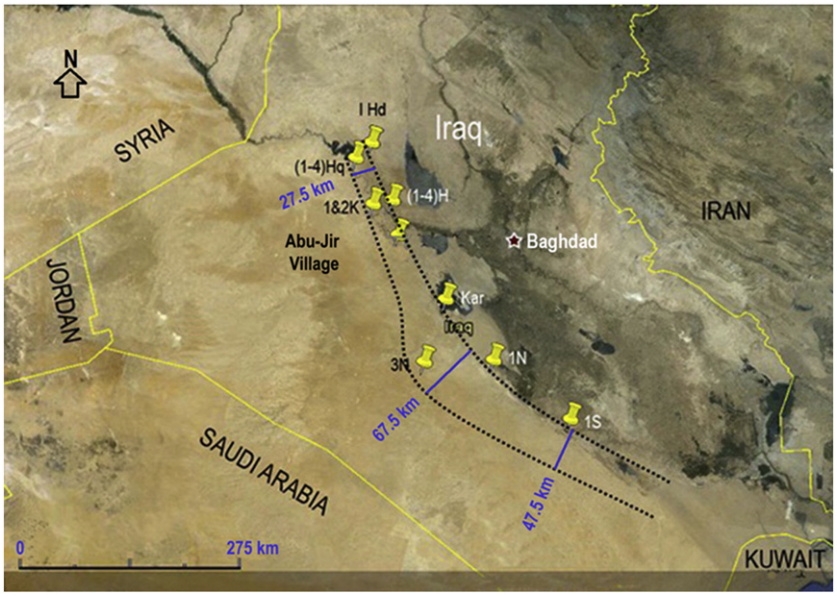

Fig. 13. Surface extension of both of width and length of the Abu-Jir Fault Zone (AJFZ) fixed on map.

seepage, springs, and similarity of local aquatic environment along the curved line from the Hadetha at the north to the Sawa Lake at the south, the surface traces of the fault zone have been clearly detected and based on the computational simulation calculated to be 467 km in length with an average width of 48 km. The computational simulation by Darcy's Law matched with the results obtained from GPS coordination of the anomaly sites of the SWS, HAGS, and GS, which were 464 km in length with an average width of 47.5 km approximately. It is possible now to represent the AJFZ on a geological map as a zone, rather than as a line. The distribution pattern of leakages of bitumen associated with the spring water, spring waters, their chemistry and geobotanical features are in harmony with the computational simulation as valid key parameters, which can be investigated in terms of geochemical exploration for estimating the surface extension of a fault zone.

Acknowledgements

We would like to thank the governorate councils of Al-Anbar and Al-Najaf for the assistance in the field work. Also our thanks go to Dr. Kamal B. Al-Hadethi for doing the chemical analyses of water in the Laboratories of the Ministry of Science and Technology. The authors express their thanks to the anonymous referees for their valuable comments, which led to a significant improvement over an early version of the paper.

References

Al-Ameri, T.K., Al-Obaydi, R.Y., 2011. Cretaceous petroleum system of the Khasib and tannuma oil reservoir, East Baghdad oil Fild, Iraq. Arabian Journal of Geosciences 4, 915–932.

Al-Ameri, T.K., Pitman, J., Naser, M.E., Zumberg, J., Al-Haydari, H.A., 2011. Programed oil generation of the Zubair Formation, Southern Iraq oil fields, results from Petromod software modeling and geochemical analysis. Arabian Journal of Geosciences 4, 1239–1259.

Al-Hajri, S., Owens, B., 2000. Stratigraphic palynology of the Paleozoic of Saudi Arabia. GeoArabia Special Publication, 1. Gulf PetrolLink, Bahrain.

Al-Rawi, F.R., Al-Ameri, T.K., Awadh, S.M., under review. Petroleum geochemistry of oil samples from shallow boreholes at Sakran site, Western Iraq. Arabian Journal of Geosciences, AJGS-S-D-12-00309, Springer.

Al-Sakini, J.A., 1992. Summary of the petroleum geology of Iraq and Middle East. Northern Oil Company Press (Naft Al-Shamal Company), Karkuk, Iraq. Report (in Arabic).

Alsharhan, A.S., kendall, C.G., 1986. Precambrian to Jurassic rocks of Arabian Gulf and Adjacent areas, their facies depositional setting and hydrocarbon habitat. American Association of Petroleum Geology Bulletin 70, 977–1002.

Alt-Epping, P., Zhao, C., 2010. Reactive mass transport modeling of a three-dimensional vertical fault zone with a finger-like convective flow regime. Journal of Geochemical Exploration 106, 8–23.

APHA, 1995. Standard methods for the examination of water and wastewater, 19th ed. American Public Health Association, Washington, DC.

API, 1996. A Guide to the Assessment and Remediation of Underground Petroleum Releases, third edition. American Petroleum Institute Publication 1628, Washington, DC.

Aqrawi, A.A., Goff, J.C., Horbury, A.D., Sadooni, F.N., 2010. The Petroleum Geology of Iraq. Scientific Press, Great Britain.

Awadh, S.M., Al-Ameri, T.K., Sahar, Y.J., Bayraktutan, S.M., 2010. Fluid inclusions used to assess oil migration in Duhok, North Iraq. Positioning, Scientefic Reserch 2, 42–49.

Bammel, B.H., Birnie, R.W., 1994. Spectral reflectance response of big sagebrush to hydrocarbon induced stress in the Bighorn Basin. Wyoming. Photogrammetic Engineering and Remote Sensing 601, 87–96.

Beck, A.E., 1981. Physical Principles of Exploration Methods, An Introduction Text for Geology and Geophysics Students. Department of Geophysics, University of Western Ontario, Macmillan.

Bellen, R.C.V., Dunnigton, H.V., Wetzel, R. Morton, D.M., 1959. Lexique Stratigraphique International, vol. III, Asie, Iraq: International Geology Congress Commission De Stratigraphique, vol. 3 Fasco 10a.

Bethke, C.M., 1985. A numerical model of compaction-driven groundwater flow and heat transfer and its application to paleohydrology of intracratonic sedimentary basins. Journal of Geophysical Research 90, 6817–6828.

Beydoun, Z.R., Futian, A.R., Jawzi, A.H., 1994. Jordan revisited of hydrocarbon habitat and petroleum. Journal of Petroleum Geology 17, 177–194.

Blyth, F.G., Fretis, M.H., 1984. A Geology for Engineers, the 7th edition by Edward Arnold. A division of Hodder and Stoughton, London, Melbourne, Auckland.

Bonnet, E., Bour, O., Odling, N.E., Davy, P., Main, I., Cowie, P., Berkowitz, B., 2001. Scaling of fracture systems in geological media. Reviews of Geophysics 39 (3), 347–383.

Buday, T., 1980. Stratigraphy and Paleogeography. In: Kassab, I.M., Jassim, S.Z. (Eds.), The Regional Geology of Iraq., 1. Geological Survey and Mineral Investigation, Baghdad, Iraq.

Childs, C., Manzocchi, T., Walsh, J.J., Bonson, C.G., Nicol, A., Schöpfer, M.P.J., 2009. A geometric model of fault zone and fault rock thickness variations. Journal of Structural Geology 31, 117–127.

Colin, E.D., 2007. Biogeochemistry in Minerals Exploration. Handbook of Exploration and Environmental Geochemistry. Elsevier, Netherlands.

Cowie, P.A., Malinverno, A., Ryan, W.B.F., Edwards, M.H., 1994. Quantitative fault studies on the East Pacific Rise: a comparison of sonar imaging techniques. Journal of Geophysical Research 99 (B8), 205–215.

Cox, S.F., 1999. Deformational controls on the dynamics of fluid flow in mesothermal gold systems. Geological Society, London, Special Publications 155, 123–139.

Dunnington, H.V., 1958. Generation, migration, accumulation and dissipation of oil in Norhthern Iraq. In: Weeks, G.L. (Ed.), Habitat of Oil, a Symposium. American Association of Petroleum Geology, Tusa.

Dunnington, H.V., Wetzel, R., Morton, D.M., 1959. Mesozoic and Paleozoic. In: Aqrawi, et al. (Ed.), The Petroleum Geology of Iraq. Scientific Press, Great Britain.

Fu, F.Q., McInnes, B.I.A., Evans, N.J., Davies, P.J., 2010. Numerical modeling of magmatic–hydrothermal systems constrained by U–Th–Pb–He time–temperature histories. Journal of Geochemical Exploration 106, 90–109.

Gessner, K., Kühn, M., Rath, V., Kosack, C., Blumenthal, M., Clauserss, C., 2009. Coupled process models as a tool for analysing hydrothermal systems. Surveys in Geophysics 30, 133–162.

Gow, P., Upton, P., Zhao, C., Hill, K., 2002. Copper–gold mineralization in the New Guinea: numerical modeling of collision, fluid flow and intrusion-related hydrothermal systems. Australian Journal of Earth Sciences 49, 753–771.

Habib, I.M., Al-Ani, T.A., Al-Mufti, M.M., 1971. Plant indicators in Iraq, native vegetation as indicators of soil salinity and water logging. Journal of Plant and Soil 34, 405–414.

Harcouët-Menou, V., Guillou-Frottier, L., Bonneville, A., Adler, P.M., Mourzenko, V., 2009. Hydrothermal convection in and around mineralized fault zones: insights from two- and three-dimensional numerical modeling applied to the Ashanti belt, Ghana. Geofluids 9, 116–137.

Harris, S.D., McAllister, E., Knipe, R.J., Odling, N.E., 2003. Predicting the three dimensional population characteristics of fault zones: a study using stochastic models. Journal of Structural Geology 25, 1281–1299.

Henson, F.R., 1950. Cretaceous and Tertiary reef formation and associated sediments in Middle East. American Association of Petroleum Geology Bulletin 34, 215–238.

Hobbs, B.E., Zhang, Y., Ord, A., Zhao, C., 2000. Application of coupled deformation, fluid flow, thermal and chemical modelling to predictive mineral exploration. Journal of Geochemical Exploration 69, 505–509.

Hodgson, C.J., 1989. The structure of shear-related, vein-type gold deposits: a review. Ore Geology Review 4, 231–273.

Jassim, S.Z., Buday, T., 2006. Tectonic framework. In: Jassm, S.Z., Goff, J.C. (Eds.), Geology of Iraq. Dolin, Prague and Moravian Museum, Brno, Czech Rebublic, pp. 45–55.

Ju, M., Zhao, C., Dai, T., Yang, J., 2011. Finite element modeling of pore-fluid flow in the Dachang ore district, Guangxi, China: implications for hydrothermal mineralization. Geoscience Frontiers 2 (3), 463–474.

Kim, Y.S., Sanderson, D.J., 2005. The relationship between displacement and length of faults. Earth-Science Reviews 68, 317–334.

Kühn, M., Dobertb, F., Gessner, K., 2006. Numerical investigation of the effect of heterogeneous permeability distributions on free convection in the hydrothermal system at Mount Isa, Australia. Earth and Planetary Science Letters 244, 655–671.

Leach, D.L., Rowan, E.L., 1986. Genetic link between Ouachita foldbelt tectonism and the Mississippi Valley-type lead-zinc deposits of the Ozarks. Geology 14, 931–935.

Lin, G., Zhao, C., Hobbs, B.E., Ord, A., Muhlhaus, H.B., 2003. Theoretical and numerical analyses of convective instability in porous media with temperature-dependent viscosity. Communications in Numerical Methods in Engineering 19, 787–799.

Lin, G., Zhou, Y., Wei, X., Zhao, C., 2006. Structural controls on pore-fluid flow and related mineralization in the Xiangshan Uranium deposit, Southern China. Journal of Geochemical Exploration 89, 231–234.

Lin, G., Zhao, C., Hobbs, B.E., Zhang, L., Zhou, Y., 2008. Potential effects of upward throughflow on thermal structure models within the continental lithospheric mantle-crust. Chinese Journal of Geophysics 51 (2), 393–401.

Lin, G., Peng, M., Zhao, C., Zhang, L., Zhang, D., Liu, S., 2009. Numerical analysis and simulation experiment of lithospheric thermal structures in the South China Sea and the Western Pacific. Journal of Earth Science 20, 85–94.

Liu, L., Yang, G., Peng, S., Zhao, C., 2005. Numerical modelling of coupled geodynamical processes and its role in facilitating predictive ore discovery: an example from Tongling, China. Resource Geology 55, 21–31.

Liu, L., Shu, Z., Zhao, C., Wan, C., Cai, A., Zhao, Y., 2008. The controlling mechanism of ore formation due to flow-focusing dilation spaces in skarn ore deposits and its significance for deep-ore exploration: examples from the Tongling-Anqing district. Acta Petrologica Sinica 24, 1848–1856.

Liu, L., Zhao, Y., Zhao, C., 2010a. Coupled geodynamics in the formation of Cu skarn deposits in the Tongling-Anqing district, China: computational modeling and implications for exploration. Journal of Geochemical Exploration 106, 146–155.

Liu, L., Zhou, R.C., Zhao, C., 2010b. Constraints of tectonic stress regime on mineralization system related to the hypabyssal intrusion: implication from the computational modeling experiments on the geodynamics during cooling process of the Yuenshan intrusion in Anqing district, China. Acta Petrologica Sinica 26 (9), 2869–2878.

Liu, L., Wan, C., Zhao, C., Zhao, Y., 2011. Geodynamic constraints on orebody localization in the Anqing orefield, China: computational modeling and facilitating predictive exploration of deep deposits. Ore Geology Reviews 43, 249–263.

Magri, F., Akar, T., Gemici, U., Pekdeger, A., 2010. Deep geothermal groundwater flow in the Seferihisar–Balçova area, Turkey: results from transient numerical simulations of coupled fluid flow and heat transport process. Geofluids 10, 388–405.

Matthai, S.K., 2003. Fluid flow and (reactive) transport in fractured and faulted rock. Journal of Geochemical Exploration 78–79, 179–182.

Matthews, M.D., Jones, V.T., Richers, D.M., 1984. Remote sensing and hydrocarbon leakage. The 3rd International Symposium: Remote Sensing of the Environment, Colorado Springs, pp. 441–450.

Mohammad, S.A.G., 2006. Megaseismic section across the northeastern slope of the Arabian plate, Iraq. GeoArabia 11 (4), 77–90.
Nield, D.A., Bejan, A., 1992. Convection in Porous Media. Springer-Verlag, New York.
Norton, D., Knight, J., 1977. Transport phenomena in hydrothermal systems: cooling plutons. American Journal of Science 277, 937–981.
Odling, N.E., 1997. Scaling and connectivity of joints systems in sandstones from western Norway. Journal of Structural Geology 19 (10), 1257–1271.
Okieimen, C.O., Okieimen, F.E., 2005. Bioremediation of crude oil-polluted soil: effect of poultry droppings and natural rubber processing sludge application on biodegradation of petroleum hydrocarbons. Environmental Sciences 12 (1), 001–008.
Oliver, J., 1986. Fluids expelled tectonically from orogenic belts: their role in hydrocarbon migration and other geologic phenomena. Geology 14, 99–102.
Oliver, N.H.S., 1995. Review and classification of structural controls on fluid flow during regional metamorphism. Journal of Metamorphic Geology 14, 477–492.
Ord, A., Hobbs, B.E., Zhang, Y., Broadbent, G.C., Brown, M., Willetts, G., Sorjonen-Ward, P., Walshe, J., Zhao, C., 2002. Geodynamic modeling of the Century deposit, Mt Isa Province, Queensland. Australian Journal of Earth Sciences 49, 1011–1039.
Patton, K.H., Manwaring, M., 1984. Evaluation of a Landsat-derived tonal anomaly for hydrocarbon microseeps, southwest Kansas. Proceeding of the 3rd International Symposium. Remote Sensing of the Environment. Colorado Springs, pp. 441–450.
Phillips, W.J., 1972. Hydraulic fracturing and mineralization. Journal of the Geological Society of London 128, 337–359.
Pollastro, R.M., Karshbaum, A.S., Viger, R.G., 1999. Map showing Geology, Oil and Gas Fields, and Geologic Provinces of the Arabian Peninsula. U.S. Geological Survey, Open File Report, version 2, 97-470B.
Powell, H.G., 1989a. Stratigarphy and sedimentation of the Phanerozoic rocks in Central and South Jordan. The Hashemite Kingdom of Jordan. Ministry of Energy and Natural resources. Geology Directorate. Geological mapping Division, Bulletin II, part A, Ram and Khreim Groups.
Powell, H.G., 1989b. Stratigarphy and sedimentation of the Phanerozoic rocks in Central and South Jordan. The Hashemite Kingdom of Jordan. Ministry of Energy and Natural resources. Geology Directorate. Geological mapping Division, Bulletin II, part B, Kurnub, Ajlun and Belqa Groups.
Pysek, P., Pysek, A., 1989. Veränderungen der Vegetation durch experimentelle Erdgasbehandlung. Weed Research 29, 193–204.
Roychoughury, S.C., Handoo, A.K., 1980. Stratigraphy and geology of oil bearing horizons in the areas around Iraq Kuwait Neutral Zone (between Iraq and Saudi Arabia) Trijunction. Geological Society of Iraq, Fifth Iraqi Geological Conference. Journal of Iraqi Geological Society 13 (1), 187–197.
Schafer, D., Schafer, W., Kinzelbach, W., 1998. Simulation of reactive processes related to biodegradation in aquifers: 1, structure of the three-dimensional reactive transport model. Journal of Contaminant Hydrology 31, 167–186.
Schaubs, P., Zhao, C., 2002. Numerical modelling of gold-deposit formation in the Bendigo-Ballarat zone, Victoria. Australian Journal of Earth Sciences 49, 1077–1096.
Schlumberger, 1991. Old sandstone new horizons. Middle East Well Evaluation Review 11, 10–26.
Schmidt, M.A., Brugger, J., Zhao, C., Schacht, U., 2010. Fluids in geological processes: the present state and future outlook. Journal of Geochemical Exploration 106, 1–7.
Schultz, R.A., Siddharthan, R., 2005. A general framework for the occurrence and faulting of deformation bands in porous granular rocks. Tectonophysics 411, 1–18.
Schultz, R.A., Soliva, R., Fossen, H., Okubo, C.H., Reeves, D.M., 2008. Dependence of displacementelength scaling relations for fractures and deformation bands on the volumetric changes across them. Journal of Structural Geology 30, 1405–1411.
Schumacher, D., 1996. Hydrocarbon-induced alteration of soils and sediments. In: Schumacher, D., Abrams, M.A. (Eds.), Hydrocarbon migration and its near-surface expression: AAPG Memoir, 66, pp. 71–89.
Sibson, R.H., 1989. Structure and Mechanics of Fault Zones in Relation to Faulthosted Mineralization. Australian Mineral Foundation, Adelaide.
Smith, K.L., Steven, M.D., Colls, J.A., 2000. Remote sensing of vegetation stress due to leaking underground gas pipelines. Aspects of Applied Biology 60, 209–212.
Sorjonen-Ward, P., Zhang, Y., Zhao, C., 2002. Numerical modeling of orogenic processes and mineralization in the south eastern part of the Yilgarn Craton, Western Australia. Australian Journal of Earth Sciences 49, 935–964.
Tedesco, S.A., 1995. Surface Geochemistry in Petroleum Exploration. Chapman and Hall, New York.
Valenta, R.K., Cartwright, I., Oliver, N.H.S., 1994. Structurally controlled fluid flow associated with breccia vein formation. Journal of Metamorphic Geology 12, 197–206.
Van der Meer, F., Van Dijk, P., Kroonenberg, S., Hong, Y., Lang, H., 2000. Hyperspectral hydrocarbon microseepage detection and monitoring: potentials and limitations. Second EARsel Workshop on Imaging Spectroscopy, Enschede, pp. 1–10.
Wang, C.Y., Beckermann, C., 1993. A two-phase mixture model of liquid–gas flow and heat transfer in capillary porous media: formulation. International Journal of Heat and Mass Transfer 36 (11), 2747–2758.
Wang, J.G., Zhang, Y., Liu, J.S., Zhang, B.Y., 2010. Numerical simulation of geofluid focusing and penetration due to hydraulic fracture. Journal of Geochemical Exploration 106, 211–218.
Weismann, T.J., 1980. Developments in geochemistry and their contribution to hydrocarbon exploration. Proceedings of the 10th World Petroleum Congress, Bucharest, Romania, 2, pp. 369–386.
Xing, H.L., Makinouchi, A., Zhao, C., 2008. Three-dimensional finite element simulation of large-scale nonlinear contact friction problems in deformable rocks. Journal of Geophysics and Engineering 5, 27–36.
Yan, Y., Lin, G., Wang, Y.J., Guo, F., Li, Z.A., Li, X.M., Zhao, C., 2003. Apatite fission track age of Mesozoic sandstones from Beipiao basin, eastern China: implications for basin provenance and tectonic evolution. Geochemical Journal 37, 377–389.
Yang, J.W., Large, R., Bull, S., Scott, D., 2006. Basin-scale numerical modeling to test the role of buoyancy driven fluid flow and heat transport in the formation of stratiform Zn-Pb-Ag deposits in the northern Mt Isa basin. Economic Geology 101, 1275–1292.
Yang, J.W., Feng, Z., Luo, X., Chen, Y., 2010. Three-dimensional numerical modeling of salinity variations in driving basin-scale ore-forming fluid flow: example from Mount Isa Basin, northern Australia. Journal of Geochemical Exploration 106, 236–243.
Zhang, Y., Hobbs, B.E., Ord, A., Barnicoat, A., Zhao, C., Lin, G., 2003. The influence of faulting on host-rock permeability, fluid flow and ore genesis of gold deposits: a theoretical 2D numerical model. Journal of Geochemical Exploration 78–79, 279–284.
Zhang, Y., Schaubs, P.M., Zhao, C., Ord, A., Hobbs, B.E., Barnicoat, A., 2008. Fault-related dilation, permeability enhancement, fluid flow and mineral precipitation patterns: numerical models. In: Wibberley, C.A.J., Kurz, W., Imber, J., Holdsworth, R.E., Collettini, C. (Eds.), The Internal Structure of Fault Zons: Implications for Mechanical and Fluid-flow Properties: Geological Society, Special Publications, London, 299, pp. 239–255.
Zhang, Y., Roberts, P., Murphy, B., 2010. Understanding regional structural controls on mineralization at the Century deposit: a numerical modeling approach. Journal of Geochemical Exploration 106, 244–250.
Zhang, L., Luo, X., Vasseur, G., Yu, C., Yang, W., Lei, U., Song, C., Yu, L., Yan, J., 2011. Evaluation of geological factors in characterizing fault connectivity during hydrocarbon migration: application to the Bohai Bay Basin. Marine and Petroleum Geology 28, 1634–1647.
Zhao, C., Mühlhaus, H.B., Hobbs, B.E., 1997. Finite element analysis of steady-state natural convection problems in fluid-saturated porous media heated from below. International Journal for Numerical and Analytical Methods in Geomechanics 21, 863–881.
Zhao, C., Hobbs, B.E., Mühlhaus, H.B., 1999. Theoretical and numerical analyses of convective instability in porous media with upward through flow. International Journal for Numerical and Analytical Methods in Geomechanics 23, 629–646.
Zhao, C., Hobbs, B.E., Mühlhaus, H.B., Ord, A., Lin, G., 2003. Convective instability of three-dimensional fluid-saturated geological fault zones heated from below. Geophysical Journal International 155, 213–220.
Zhao, C., Hobbs, B.E., Ord, A., Peng, S., Mühlhaus, H.B., Liu, L., 2004. Theoretical investigation of convective instability in inclined and fluid-saturated three-dimensional fault zones. Tectonophysics 387, 47–64.
Zhao, C., Hobbs, B.E., Hornby, P., Ord, A., Peng, S., 2006. Numerical modeling of fluids mixing, heat transfer and non-equilibrium redox chemical reactions in fluid-saturated porous rocks. International Journal for Numerical Methods in Engineering 66, 1061–1078.
Zhao, C., Hobbs, B.E., Ord, A., Hornby, P., Peng, S., Liu, L., 2007. Mineral precipitation associated with vertical fault zones: the interaction of solute advection, diffusion and chemical kinetics. Geofluids 7, 3–18.
Zhao, C., Hobbs, B.E., Ord, A., 2008a. Convective and Advective Heat Transfer in Geological Systems. Springer, Berlin.
Zhao, C., Hobbs, B.E., Ord, A., 2008b. Investigating dynamic mechanisms of geological phenomena using methodology of computational geosciences: an example of equal-distant mineralization in a fault. Science in China Series D: Earth Sciences 51, 947–954.
Zhao, C., Hobbs, B.E., Hornby, P., Ord, A., Peng, S., Liu, L., 2008c. Theoretical and numerical analyses of chemical-dissolution front instability in fluid-saturated porous rocks. International Journal for Numerical and Analytical Methods in Geomechanics 32, 1107–1130.
Zhao, C., Hobbs, B.E., Ord, A., 2009. Fundamentals of Computational Geoscience: Numerical Methods and Algorithms. Springer, Berlin.
Zhao, C., Hobbs, B.E., Ord, A., 2010. Theoretical and numerical investigation into roles of geofluid flow in ore forming systems: integrated mass conservation and generic model approach. Journal of Geochemical Exploration 106, 251–260.
Zhao, C., Reid, L.B., Regenauer-Lieb, K., 2012. Some fundamental issues in computational hydrodynamics of mineralization: a review. Journal of Geochemical Exploration 112, 21–34.